Strong-coupling expansions and phase diagrams for the O(2), O(3), and O(4) Heisenberg spin systems in two dimensions

C. J. Hamer
University of Melbourne, Parkville, Victoria 3052, Australia

John B. Kogut
Department of Physics, University of Illinois at Urbana-Champaign, Urbana, Illinois 61801

L. Susskind
Stanford University, Stanford, California 94305

(Received 16 October 1978)

The Ising and O(n), $2 \leq n \leq 4$, models in two dimensions are studied using a quantum-mechanical Hamiltonian formalism in which a "time" axis is continuous and a spatial axis is discrete. Strong-coupling series for the theory's mass gaps and β (Callan-Symanzik) functions are computed and are used to search for phase transitions. The critical point and critical index ν of the Ising model are found exactly. The critical point of the O(2) model is found ($g^* = 1.08$), and the series suggest that the theory's correlation length possesses an essential singularity with the behavior predicted by Kosterlitz. The critical points of the O(3) and O(4) models are predicted to be at zero coupling, i.e., no evidence for a phase transition at nonzero g is found for the non-Abelian models. Interpolating forms (two-point Padé approximants) for these theories' β (Callan-Symanzik) functions are computed for all g. The transition regions between weak and strong coupling are seen to be quite narrow.

I. INTRODUCTION

There is renewed interest among field theorists and statistical mechanicians to understand the phase diagrams of two-dimensional spin systems. It is the purpose of this paper to present some results for these models, which we have obtained using methods originally devised for calculating the mass spectra of non-Abelian gauge theories in 3+1 dimensions.[1] Before delving into the particulars of our analyses, we will briefly review the theoretical issues of interest.

Consider the O(2), O(3), and O(4) Heisenberg models in two dimensions. These systems have been studied using high-temperature expansions, perturbation theory (low-temperature expansions), real-space renormalization-group methods, etc. The high-temperature expansions[2] have not yielded much insight or reliable results. They suggest that each model undergoes a phase transition at a finite temperature. Such a phase transition would have to be quite delicate since rigorous theorems prove that it could not be accompanied by the appearance of a spontaneous magnetization.[3] It is commonly believed that a transition does occur for the O(2), planar Heisenberg, model in light of the fundamental work done by Kosterlitz and Thouless.[4] These authors argued for a simple physical picture of the phases of the model. Roughly speaking, there is a low-temperature phase where spin waves are the only relevant excitations in the system. They are responsible for the vanishing of the system's magnetization and lead to a power-behaved spin-spin correlation function [i.e., $\langle \vec{s}(0) \cdot \vec{s}(\vec{r}) \rangle \sim |\vec{r}|^{-p}$ where p is a temperature-dependent exponent]. There is a phase transition at a sufficiently high temperature T_c above which new excitations, vortices, occur with finite probability. They completely disorder the system producing a spin-spin correlation function which falls off exponentially with the distance between the spins. Kosterlitz[5] has derived renormalization-group equations for the model which describe the detailed behavior of its critical region. (Some of his results will be cited and used for comparison later in this article.)

The theoretical analyses of the O(n) models for $n \geq 3$ are less complete. Polyakov[6] made the crucial observation that these models are "asymptotically free", i.e., the temperature $T = 0$ is an infrared-unstable fixed point. This perturbative result has suggested to many authors that these theories possess only one phase and that a correlation length, which depends nonanalytically on T, is generated dynamically so that the spin-spin correlation function falls exponentially for *all* T. A real-space renormalization group due to Migdal[7] does, in fact, lead to these results. His method also reproduces the low-temperature perturbation-theory analysis done by Polyakov[6] and others[8] to good accuracy. Further evidence for the correctness of the idea that the O(3) and O(4) models have only a high-temperature phase comes from the solution for the S matrices of these models.[9] It has been

found that the assumption of a dynamically generated mass leads to a consistent S matrix for $n \geq 3$. Although the multispin correlation functions have not been obtained explicitly, these S-matrix results indicate that the correlation functions fall off exponentially in the distance between any two spins.

The $O(n)$ spin systems are particularly interesting because they are thought to have many properties in common with lattice gauge theories in four dimensions.[6] The likely result that all the $O(n)$ models for $n \geq 3$ possess only a high-temperature phase is thought to map into the property that non-Abelian gauge theories confine quarks and are asymptotically free. The Migdal recursion relation lends credence to this possibility because it gives the same renormalization group for an $SU(n) \times SU(n)$ spin system in two dimensions as an $SU(n)$ lattice gauge theory in four dimensions.[7,10] The $O(3)$ spin system has another special property first emphasized by Polyakov.[11] This model contains instantons—finite-action, topologically stable spin configurations—which tend to disorder the system but are probably not sufficient to generate exponentially damped correlation functions. All non-Abelian gauge theories in four dimensions contain instantons which enhance the quark-quark potential but do not lead to confinement. Since the Heisenberg spin systems are probably soluble,[12] there even exists the hope that non-Abelian gauge theories in four dimensions are soluble.

Theoretical physics is far from establishing this dream. In this paper we will investigate with very limited tools just a few questions which are important hurdles in this program. We shall search for phase transitions in the Hamiltonian lattice version (discrete space, continuous time) of these spin systems by developing strong-coupling expansions for each theory's mass gap. We shall find strong evidence for a phase transition in the $O(2)$ model and will estimate the critical coupling using several methods of analysis including the ratio test and Padé approximants. Our series expansion also suggest that the mass gap has an essential singularity in the critical region in agreement with Kosterlitz's renormalization group.[5] We find strong evidence for the *absence* of a phase transition in the $O(3)$ and $O(4)$ models. This result is in agreement with contemporary prejudice and in apparent disagreement with standard strong-coupling expansions based on the isotropic spin models and the partition function.[2] We believe that the Hamiltonian strong-coupling expansion is a better guide to the phases of these models than the tranditional expansion method because it begins with one space-time axis continuous. This feature makes it particularly sensitive to second- (or higher-) order phase transitions which are signaled by the appearance of long-range correlations. The expansion coefficients of the non-Abelian models are distinctly different from those of the Abelian model. In fact, we shall extrapolate our non-Abelian model results to weak coupling and find excellent numerical matches with standard perturbation theory. As a warm-up we also carry out such calculations for the Ising model in a transverse field. In this case the strong-coupling expansion truncates and the critical coupling constant is determined *exactly*.

One purpose of this article is to sharpen our techniques and test them before pursuing other more challenging exercises in lattice gauge theories in more spatial dimensions.

In the later sections of this article the models and our calculations are presented in detail. Some discussion and related questions appear in a closing section.

II. QUANTUM LATTICE HAMILTONIAN FORMALISM FOR TWO-DIMENSIONAL SPIN SYSTEMS

A. O(2) quantum Hamiltonian

Consider the planar Heisenberg or $O(2)$ model as an example. The standard statistical-mechanics formulation of the model places two-component unit vectors $\vec{n}$ or a two-dimensional square array of lattice sites $\vec{m}$. Nearest-neighbor spins are coupled through their inner product so the Hamiltonian is

$$H = -K \sum_{\vec{m},\vec{\mu}} \vec{n}(\vec{m}) \cdot \vec{n}(\vec{m}+\vec{\mu}), \tag{2.1}$$

where the set $\{\vec{\mu}\}$ consists of the two independent unit lattice vectors and $K = J/kT$. The spin vectors $n(\vec{m})$ can be parametrized as

$$\vec{n}(\vec{m}) = (\cos\theta(\vec{m}), \sin\theta(\vec{m})) \tag{2.2}$$

and the spin configurations can be visualized as an array of planar unit vectors. It is frequently more convenient to write Eq. (2.1) in the form

$$H = \tfrac{1}{2}K \sum_{\vec{m},\vec{\mu}} [\vec{n}(\vec{m}) - \vec{n}(\vec{m}+\vec{\mu})]^2, \tag{2.3}$$

where an irrelevant constant term has been dropped. In this form it is clear that the classical continuum limit (let the lattice spacing a go to zero) of the Hamiltonian is

$$H = \tfrac{1}{2}K \int d^2x \left[\sum_{i=1,2} \nabla_i \vec{n}(x) \cdot \nabla_i \vec{n}(x) \right]. \tag{2.4}$$

The relativistic field theory corresponding to Eq. (2.4) is obtained by making a Wick rotation. Then $x_1 \to it$, $x_2 \to x$ which replaces the Euclidean metric by the Minkowski metric, and replaces the statistical-mechanics Hamiltonian H by the action S,

$$H \to -iS, \tag{2.5}$$

where

$$S = \frac{1}{2g} \int dt\, dx (\partial_\mu \vec{n} \cdot \partial^\mu \vec{n})$$

and we have replaced K by $1/g$ to conform with standard notation.[8] The Lagrangian density of the model is that of the O(2) σ model,

$$\mathcal{L} = \frac{1}{2g} \partial_\mu \vec{n} \cdot \partial^\mu \vec{n}, \quad n^2(x) = 1. \tag{2.6}$$

Using the parametrization for the spin variable given in Eq. (2.2),

$$\mathcal{L} = \frac{1}{2g} [\dot{\theta}^2 - (\partial_x \vec{n})^2], \quad 0 \leq \theta \leq 2\pi \tag{2.7}$$

which is a convenient form for the passage to the quantum-mechanical Hamiltonian. The variable conjugate to θ is

$$\frac{\partial \mathcal{L}}{\partial \dot{\theta}} = \frac{1}{g} \dot{\theta}, \tag{2.8}$$

so the Hamiltonian density is

$$\mathcal{H} = \frac{1}{2g} [\dot{\theta}^2 + (\partial_x \vec{n})^2]. \tag{2.9}$$

Finally, consider the theory with a discrete spatial axis but a *continuous* temporal axis. It is clear from Eq. (2.9) that the Hamiltonian for such a physical system is

$$H = \frac{a}{2g} \sum_m \left[\dot{\theta}(m)^2 - \frac{2}{a^2} \vec{n}(m) \cdot \vec{n}(m+1)\right], \tag{2.10}$$

where the integer m labels the spatial lattice and a is the lattice spacing. It is this form of the theory which will be used below to generate strong-coupling expansions. The first term in Eq. (2.10) can be recognized as a rotational energy term "$\frac{1}{2}I\omega^2$," "where the moment of inertia per site" $I = a/g$. Therefore, the spin angular momentum per site is

$$J(m) = \frac{a}{g} \dot{\theta}(m). \tag{2.11}$$

The Hamiltonian can now be written in a particularly convenient form,

$$H = \frac{g}{2a} \sum_m [J^2(m) - x\vec{n}(m) \cdot \vec{n}(m+1)], \tag{2.12}$$

where

$$x = 2/g^2.$$

Finally, we need the commutation relations of $J(m)$ and $\vec{n}(m')$. It follows from Eqs. (2.8) and (2.11) that

$$[J(m), e^{\pm i\theta(m')}] = \pm e^{\pm i\theta(m')} \delta_{m,m'}. \tag{2.13}$$

It is therefore slightly more convenient to replace $\vec{n}(m)$ by the phase variables $\exp[\pm i\theta(m)]$,

$$\phi(m) \equiv e^{+i\theta(m)} = n_1(m) + i n_2(m) \tag{2.14}$$

and write Eq. (2.12) as

$$H = \frac{g}{2a} \sum_m \left\{J^2(m) - \frac{x}{2} [\phi^\dagger(m)\phi(m+1) + \text{H.c.}]\right\}. \tag{2.15}$$

The value of writing H in this form, as opposed to Eq. (2.10), is that each term has a magnitude which is simple to estimate. Since $J(m)$ is an angular momentum which generates planar rotations, it has a discrete spectrum which consists of the integers. And since the spins $\vec{n}(m)$ are unit vectors, the second term in Eq. (2.15) is at most x per link.

There are many different ways to arrive at Eq. (2.15) starting with Eq. (2.1), say. One might define the transfer matrix for the statistical-mechanics formulation, take the continuum limit on the "time" axis, and identify the generator of these translations as the quantum-mechanical Hamiltonian Eq. (2.15). This approach is described in Refs. 13 and 14.

B. Strong-coupling expansions for eigenvalues

Our next task is to form a perturbation series in $x(=2/g^2)$ for the eigenvalues of the Hamiltonian Eq. (2.15). This is a "strong-coupling expansion" ($x \to 0$ implies $g \to \infty$) which is closely related to the high-temperature expansion of the partition function of the tranditional statistical-mechanics formulation of the model.[15] The relation between the methods is nontrivial, however, since they employ very different cutoff procedures—in one case space and time are handled symmetrically and in the other case the time continuum limit is taken at the start. The contrast between the two methods is clearest when the quantum Hamiltonian is obtained from the statistical-mechanics Hamiltonian via the transfer matrix. The practical differences between the methods will be clear to the experienced statistical mechanician from the calculations which will be discussed below. Of course, both methods should describe the same physics, i.e., the critical phenomena of the two-dimensional spin systems should be independent of their detailed lattice structure. However, as will be discussed further below, given a finite amount of work, the quantum-mechanical Hamiltonian appears to be more efficient at uncovering the phases of each model.

To develop the strong-coupling expansion it is convenient to define the dimensionless operator

$$W \equiv \frac{2a}{g} H \equiv W_0 - xV, \tag{2.16}$$

where

$$W_0 = \sum_m J^2(m) \tag{2.17}$$

and

$$V = \tfrac{1}{2} \sum_m [\phi^\dagger(m)\phi(m+1) + \text{H.c.}]. \tag{2.18}$$

The diagonalization of W_0 is trivial since it does not couple different lattice sites. The operator xV can, therefore, be treated as a perturbation on an exactly soluble problem and all the well-established techniques of Hamiltonian perturbation theory can be brought to bare on the problem.

We shall consider the ground state and first excited state of the model in detail. The ground state of W_0, which we denote $|0\rangle$, is that for which

$$J^2(m)|0\rangle = 0 \tag{2.19}$$

for all m. The lowest-energy, translationally invariant state is the zero-momentum state of a spin wave,

$$|1\rangle = \frac{1}{\sqrt{M}} \sum_{m=1}^{M} \phi^\dagger(m)|0\rangle, \tag{2.20}$$

where M is the number of links in the spatial lattice.

The effect of V on the energies of the states $|0\rangle$ and $|1\rangle$ has been calculated to *eighth* order in x. This was done by machine and considerable checks were made on the calculation by hand. We shall illustrate a few very simple calculations here. First note that the effect of V is to raise the spin at one site by a unit and lower it at a neighboring site. So, if we represent a spin +1 (−1) at a site by an upward (downward) pointing arrow, then the state $|1\rangle$ can be represented as in Fig. 1(a). The first-order term in the perturbation expansion of the W eigenvalue of $|1\rangle$, V_{11}, is then represented as in Fig. 1(b). So, to order x, ω_1, the W eigenvalue of $|1\rangle$, is

$$\omega_1 = 1 - 2\left(\frac{x}{2}\right) + O(x^2). \tag{2.21}$$

The first nonvanishing contribution to the ground state ω_0 is the second-order term shown in Fig. 1(c). Since the W_0 value of the intermediate state is 2, we have

$$\omega_0 = 0 + \left(\frac{x}{2}\right)^2 \frac{2M}{(-2)} + O(x^4). \tag{2.22}$$

The factor M accounts for the fact that the vacuum fluctuations can appear on any link and it insures that the vacuum energy is proportional to the volume of space. The quantity of most interest to us is the "mass gap," the energy of the first excited state relative to the vacuum,

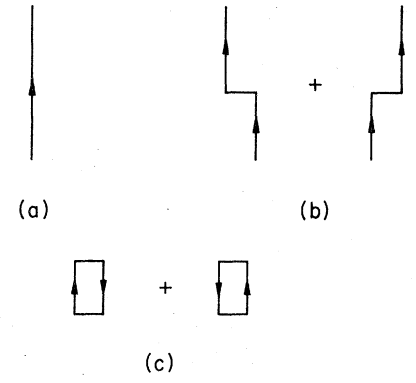

FIG. 1. (a) Flipped spin on a single site, (b) the potential V moves the flipped spin one lattice site, (c) second-order corrections to the ground state.

$$W - \text{gap} = \omega_1 - \omega_0. \tag{2.23}$$

The expansion coefficients for these quantities are recorded in Table I. To proceed to eight order the computer first generated orthonormal spin eigenstates order by order in x by iteration of the perturbation operator V_{ij} between them. The initial-state eigenvalues could then be computed by standard formulas. This method of computation is equivalent to but somewhat more efficient than evaluating the Raleigh-Schrödinger perturbation series directly.[15]

The physics in these series will be discussed below after the other models of interest have been introduced.

C. Other spin systems

The formulation of the O(3) and O(4) Heisenberg models can be done in precisely the same way as for the O(2) model with the obvious generalizations to account for the higher spin dimensionality. The results are as follows:

1. O(3) model

The quantum-mechanical lattice Hamiltonian reads

$$H = \frac{g}{2a} \sum_m [\vec{J}^2(m) - x\vec{n}(m)\cdot\vec{n}(m+1)], \tag{2.24}$$

where $x = 2/g^2$ as usual, $\vec{J}$ is a three-component angular momentum, and $\vec{n}(m)$ is a three-component spin. The commutation relations of $\vec{J}$ and $\vec{n}$ are the familiar ones of the rotation groups in three dimensions. The most convenient spin variables are

TABLE I. Strong-coupling series expansion coefficients for the Ising, O(2), O(3), and O(4) spin models. Expansions are given for the ground-state energy per site, ω_0/N; for the "mass gap" to the first excited state, $\omega_1-\omega_0$; and for the β function, $\beta(g)/g$, defined in the text. The expansion parameter in all cases is $x=2/g^2$.

Order	Ising model		O(2) model		
	ω_0/M	$\omega_1-\omega_0$	ω_0/M	$\omega_1-\omega_0$	$\beta(g)/g$
0	0	2	0	1	1
1	0	−2	0	−1	−2
2	−0.25	0	−0.25	0.125	2.5
3	0	0	0	0.031 25	−3.0625
4	−0.015 625	0	$6.510\,417\times10^{-3}$	$1.438\,802\times10^{-2}$	3.8026
5	0	0	0	$6.002\,063\times10^{-3}$	−4.7018
6	$-3.906\,25\times10^{-3}$	0	$1.220\,445\times10^{-3}$	$2.261\,48\times10^{-4}$	5.7958
7	0	0	0	$6.957\,99\times10^{-4}$	−7.1334
8	$-1.525\,88\times10^{-3}$	0	$1.813\,093\times10^{-5}$	-1.752×10^{-4}	8.7760

Order	O(3) model			O(4) model		
	ω_0/M	$\omega_1-\omega_0$	$\beta(g)/g$	ω_0/M	$\omega_1-\omega_0$	$\beta(g)/g$
0	0	2	1	0	3	1
1	0	−0.66	−0.66	0	−0.5	−0.33
2	−0.083	$3.703\,70\times10^{-2}$	0.296 30	−0.041 6	0.015 625	7.6389×10^{-2}
3	0	$4.320\,988\times10^{-3}$	−0.122 84	0	$1.139\,323\times10^{-3}$	-1.5661×10^{-2}
4	$5.787\,04\times10^{-4}$	$3.274\,22\times10^{-4}$	$5.151\,6\times10^{-2}$	$9.817\,295\times10^{-5}$	$1.252\,19\times10^{-5}$	3.2042×10^{-3}
5	0	$2.014\,046\times10^{-5}$	$-2.145\,9\times10^{-2}$	0	$-1.082\,289\times10^{-6}$	-6.4704×10^{-4}
6	$2.764\,367\times10^{-6}$	$-1.688\,199\times10^{-5}$	$8.865\,9\times10^{-3}$	$-9.541\,727\times10^{-8}$	$-7.567\,09\times10^{-7}$	1.2846×10^{-4}

$$\sigma_{\pm1}(m)=\frac{1}{\sqrt{2}}\left[\mp n_1(m)-i\,n_2(m)\right],\quad \sigma_0(m)=n_3(m) \tag{2.25}$$

appropriate to a basis in which $J^2(m)$ and $J_3(m)$ are simultaneously diagonalized at each site. The hopping term in Eq. (2.24) then has the form

$$\vec{n}(m)\cdot\vec{n}(m+1)=\sum_{i=\pm1,0}(-1)^i\sigma_{-i}(m)\sigma_i(m), \tag{2.26a}$$

where

$$\sigma_i(m)=\left(\frac{4\pi}{3}\right)^{1/2}Y_{1i}(\theta(m),\phi(m)) \ . \tag{2.26b}$$

The strong-coupling expansions for the model have the same structure as for the O(2) model but now one must also compute group-theoretic weights for the graphs. In addition, there are graphs in the non-Abelian systems that have no Abelian counterpart. An example that occurs in third order is shown in Fig. 2. The group-theoretic weights are easily computed in terms of Clebsch-Gordan coefficients or Racah coefficients. In our computer calculations Eq. (2.26) and the reduced matrix element[16]

$$(J_f\|\sigma\|J_i)=\langle J_i100\,|\,J_i1J_f0\rangle\left(\frac{2J_i+1}{2J_f+1}\right)^{1/2} \tag{2.27}$$

were sufficient for our purposes.

2. O(4) model

The quantum-mechanical Hamiltonian has the form

$$H=\frac{g}{2a}\sum_m\left[\vec{J}^2(m)-x\,\vec{n}(m)\cdot\vec{n}(m+1)\right], \tag{2.28}$$

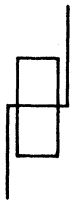

FIG. 2. Intrinsically non-Abelian graph.

where $x=2/g^2$. Now $\vec{n}$ has four components and $\vec{J}$ has six [The generators of O(4)]. There are two convenient ways of dealing with these variables. Since $O(4)=SU(2)\otimes SU(2)$, one can use Pauli matrix technology. Alternatively, following the discussion of the O(3) model rather closely, one can use O(4) spherical harmonics. Following Biedenharn's notation,[17] one can diagonalize four components of $\vec{J}$ at each site: P, Q, L, and M with $Q\equiv 0$ for the representations we are concerned with. The spectrum of J^2 is $P(P+2)$ with $P=0,1,2,\ldots$. The spin variables can be written

$$\sigma_{1,\pm1}(m)=\frac{1}{\sqrt{2}}[\mp n_1(m)-in_2(m)]$$
$$=\left(\frac{2\pi^2}{4}\right)^{1/2}Y_{2,1,\pm1}(\theta_1(m),\theta_2(m),\phi(m))\,, \tag{2.29}$$
$$\sigma_{1,0}(m)=n_3(m)=\left(\frac{2\pi^2}{4}\right)^{1/2}Y_{2,1,0}(\theta_1(m),\theta_2(m),\phi(m))\,,$$
$$\sigma_{0,0}(m)=n_4(m)=\left(\frac{2\pi^2}{4}\right)^{1/2}Y_{2,0,0}(\theta_1(m),\theta_2(m),\phi(m))\,,$$

where the Y_{nlm} are the O(4) spherical harmonics. Then,

$$\vec{n}(m)\cdot\vec{n}(m+1)=\sum_{l=0,1}\sum_{i=-(2l+1)}^{2l+1}(-1)^{l-i}\sigma_{l,-i}(m)\sigma_{l,i}(m+1) \tag{2.30}$$

and the symmetry coefficients needed for the strong-coupling expansions are

$$\langle P0LM|\sigma_{lm}|P'0L'M'\rangle=(P+1)(P'+1)[(2l+1)(2L'+1)]^{1/2}\langle lL'M'm|lL'LM\rangle \begin{Bmatrix} \frac{1}{2} & \frac{1}{2} & \frac{P}{2} \\ \frac{1}{2} & \frac{1}{2} & \frac{P}{2} \\ L' & l & L \end{Bmatrix} \begin{Bmatrix} \frac{P'}{2} & \frac{1}{2} & \frac{P}{2} \\ \frac{P'}{2} & \frac{1}{2} & \frac{P}{2} \\ 0 & 0 & 0 \end{Bmatrix}, \tag{2.31}$$

where the curly brackets are Racah (6-j) symbols.[18]

3. *Ising model*

Although this model does not address the theoretical issues of interest here, it is soluble and provides a good test for our methods. The quantum-mechanical Hamiltonian for the Ising model of statistical-mechanics fame is

$$H=\frac{g}{2a}\left(\sum_m[1-\sigma_3(m)]-x\sum_m\sigma_1(m)\sigma_1(m+1)\right), \tag{2.32}$$

where the $\sigma_i(m)$ are the usual Pauli matrices. We have arranged the Hamiltonian so that in the strong-coupling limit (which corresponds to the high-temperature limit of the Ising model), all spins are pointing up,

$$\sigma_3(m)=+1\,. \tag{2.33}$$

The perturbation expansions of the ground-state W-energy per site (ω_0/M) and the W-mass gap to the first excited state ($\omega_1-\omega_0$) are listed in Table I with the results for the other models. Note that the W-mass gap series *truncates* after first order, and we have precisely

$$\omega_1-\omega_0=2(1-x)\,. \tag{2.34}$$

This result agrees with the exact solution[19] of the model. The mass gap vanishes linearly at $x=1$, the critical point singled out by the self-duality of the model.[14] This model constitutes an example of a theory whose mass gap depends on the expan-

sion parameter in such a simple (polynomial) form, that the strong-coupling expansion can (and must) provide the *exact* answer.

III. RENORMALIZATION OF THE COUPLING, THE β FUNCTION, AND PHASE DIAGRAMS

We wish to use our expansions discussed in the previous section to search for possible phase transitions in these models as x varies. This was particularly trivial for the Ising model since the equation for the mass gap was found exactly. The gap vanished at $x=1$ indicating the presence of a massless particle and long-range correlations. At $x=1$ the continuum limit of the model can be taken and one retrieves the field theory of a free massless fermion.[19]

For models more complicated than the Ising model, one needs more sophisticated methods of searching for phase transitions. It is often best not to use the expansion for the mass gap directly because that quantity carries dimensions $(1/a)$ and usually has a complicated dependence on the expansion parameter. Instead one considers the β function,

$$\beta(g)=a\,\frac{dg}{da}\,. \tag{3.1}$$

The meaning of Eq. (3.1) is the following: Consider the mass of the first excited state of any of the spin systems of interest,

$$E=\frac{g}{2a}\,(\omega_1-\omega_0)\equiv\frac{g}{2a}\,F(x)\,. \tag{3.2}$$

Since the lattice and its spacing "a" simply provide the scaffolding on which to define the theory, one can imagine changing a. But we also wish each formulation of the theory to generate the same physics, i.e., in physical units (GeV, say) E should be independent of a,

$$\frac{dE}{da}=0\,. \tag{3.3}$$

This renormalization condition implies that the physics will be indpendent of a only if g depends on a in a definite fashion. Substituting Eq. (3.2) into Eq. (3.1) we find, in fact,

$$\frac{\beta(g)}{g}=\frac{F(x)}{F(x)-2xF'(x)}\,. \tag{3.4}$$

Since we have the strong-coupling expansion for $F(x)$, the expansion for β can be obtained in this way. We note in addition that the vanishing of F implies the vanishing of β, so a search for zeros in the series for β is the same as the search for a vanishing mass gap (continuous phase transition). In addition, the weak-coupling (small g) expansions for β are known in many cases. Given this information and our strong-coupling expansions, a fairly thorough search for phase transitions can be made.

IV. SEARCH FOR PHASE TRANSITIONS

We will use several different methods of analyzing the series of Table I in our quest for zeros of β. We begin by testing for a power-law zero in the mass gap,

$$F(x)\underset{x\to x_c}{\sim}b(x_c-x)^{\rho}\,, \tag{4.1}$$

at the point $x=x_c$. From Eq. (3.4) this would imply a first-order zero for $\beta(g)$,

$$\frac{\beta(g)}{g}\underset{x\to x_c}{\sim}\frac{1}{2\rho x_c}\,(x_c-x)\,. \tag{4.2}$$

A. The ratio test

We briefly remind the reader of this method of testing for the tendency of a series to develop a singularity. If a function

$$f(x)=\sum_{n=0}^{\infty}a_n x^n \tag{4.3}$$

has a power-law singularity at $x=x_c$,

$$f(x)\underset{x\to x_c}{\sim}b(x-x_c)^{-\rho}\,, \tag{4.4}$$

then the ratio of successive coefficents should obey the law

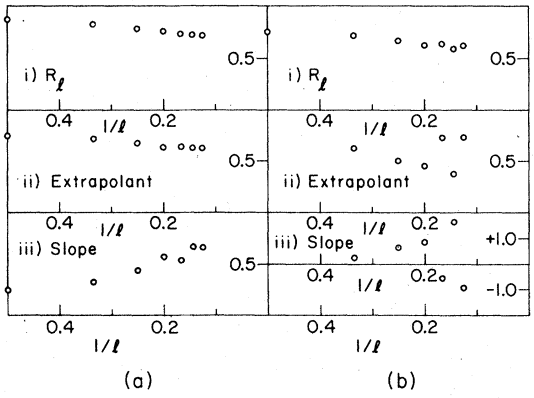

FIG. 3. Results of the ratio test applied to (a) the inverse mass gap, $[F(x)]^{-1}$; and (b) the inverse β function, $[\beta(g)/g]^{-1}$, for the O(2) model. In each case, we plot (i) R_l vs $1/l$; (ii) the first-order linear extrapolant of R_l vs $1/l$; and (iii) the slope of R_l curve vs $1/l$.

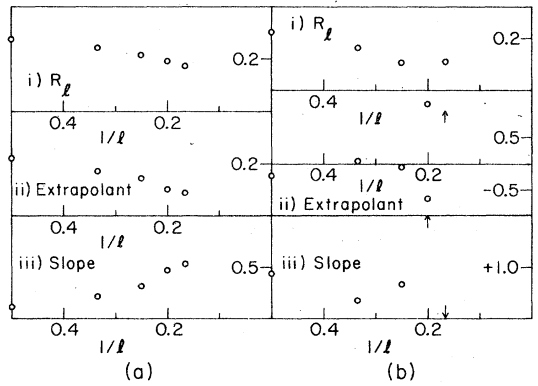

FIG. 4. Same as Fig. 3, for the O(3) model.

$$R_l \equiv a_l/a_{l-1} \underset{l\to\infty}{\sim} x_c^{-1}\left(1+\frac{\rho-1}{l}\right). \tag{4.5}$$

So, if R_l is plotted against $1/l$, both the critical coupling x_c and the critical index ρ can be determined.

This test has been applied to the inverse mass gap $[F(x)]^{-1}$, and the inverse β function, $[\beta(g)/g]^{-1}$, for the O(2), O(3), and O(4) models. The results are shown in Figs. 3, 4, and 5, respectively. In these figures we have plotted in each case

(i) R_l vs $1/l$;

(ii) the first-order linear extrapolant, $lR_l - (l-1)R_{l-1}$ vs $1/l$ which gives an estimate of the intercept x_c^{-1};

(iii) the slope, $(R_l - R_{l-1})/[1/l - 1/(l-1)]$, which gives an estimate of $x_c^{-1}(\rho-1)$ and hence the critical index ρ.

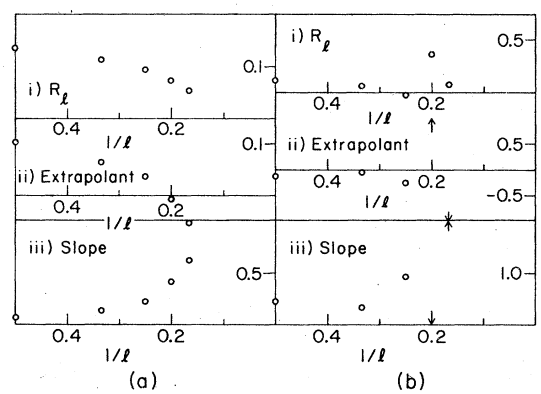

FIG. 5. Same as Fig. 3, for the O(4) model.

The results are as follows:

1. O(2) model

The ratios of $[F(x)]^{-1}$ show strong evidence of a phase transition. The linear extrapolants converge nicely, giving an estimate of the critical point,

$$x_c = 1.6 \pm 0.3. \tag{4.6}$$

The convergence of the slopes, however, is slow. Our best guess for the critical index (assuming a power-behaved gap) ρ is

$$\rho = 2.0 \pm 0.5 \tag{4.7}$$

from the values at higher l. This value for ρ should not be taken very seriously since there is a tendency for the values to rise with increasing l. This suggests that the assumption of a power-behaved gap is not correct. Below we shall investigate other possible functional forms for F.

The ratios for $[\beta(g)/g]^{-1}$ also show strong evidence for a phase transition, although the series is not as quickly convergent as that for $[F(x)]^{-1}$. We estimate

$$x_c = 1.7 \pm 0.6 \tag{4.8}$$

from this test. The plot of the slopes shows no sign of convergence,[20] so a value for ρ', the order of β's zero at x_c, cannot be determined.

2. O(3) model

Figure 4 is particularly interesting. The ratios for $[F(x)]^{-1}$ show *no* evidence of a phase transition. The linear extrapolants are positive, but are moving rapidly downwards with increasing l—they show no sign of convergence to any positive value. The slopes are consistently increasing with l, and also show no sign of convergence.

The ratios for $[\beta(g)/g]^{-1}$ are again more slowly convergent. There is no evidence of a singularity at any finite x, but it might be argued that the linear extrapolants (excepting the last two) are close to zero, indicating the possibility of a singularity at $x\to\infty$. Of course, the β function is known to vanish there so this is a welcome result.

3. O(4) model

This model behaves similarly to the O(3) model. The linear extrapolants for $[F(x)]^{-1}$ actually drop below zero, providing strong evidence *against* a phase transition. Again the extrapolants of $[\beta(g)/g]^{-1}$ are consistent with a singularity [a zero of $\beta(g)/g$] at $x\to\infty$ (Fig. 5).

TABLE II. The positions and residues (in brackets) of poles on the positive, real x axis in Padé approximants for the O(2) model. The functions approximated are (a) the logarithmic derivative of $F(x)$, the mass gap; and (b) the logarithmic derivative of $\beta(g)/g$, the β function. The [4, 3] approximant in part (a) is not reliable since there is a spurious pole closer to the origin. Also, the [3, 4] approximant in part (a) exhibits another nearby pole [at 2.30 (−2.9)] so its high residue is not significant.

	(a)				(b)		
N	$[N/N-1]$	$[N/N]$	$[N/N+1]$	N	$[N/N-1]$	$[N/N]$	$[N/N+1]$
0			1.33(1.33)	0			•••
1		1.41(1.49)	•••	1		•••	1.66(1.36)
2	1.52(1.88)	•••	1.34(1.24)	2	•••	2.01(2.25)	1.85(1.72)
3	1.59(2.21)	1.63(2.49)	1.71(3.84)	3	1.72(1.28)	1.52(0.67)	1.80(1.59)
4	1.52(2.90)			4	1.70(1.22)		

4. *Ising model*

Since the series truncate we obtain exact results in this case. The ratios for $[F(x)]^{-1}$ are $R_l \equiv 1$, giving $x_c = 1$ and $\rho = 1$ exactly.

We now turn to a second, standard method of extracting information from strong-coupling expansions.

B. The Padé-approximant test

We begin by illustrating the method. Consider a function with an algebraic zero at some point x_c,

$$g(x) \underset{x \to x_c}{\sim} b(x_c - x)^{\gamma} . \tag{4.9}$$

Then the function's logarithmic derivative has a simple pole at that point,

$$\frac{d}{dx} \ln g(x) = \frac{g'(x)}{g(x)} \underset{x \to x_c}{\sim} \frac{\gamma}{(x - x_c)} . \tag{4.10}$$

By forming Padé approximants to the logarithmic derivative, we may estimate both the position and residue of any pole and read off the critical point x_c and the critical index γ. We have applied this test to the logarithmic derivatives of $F(x)$ and $\beta(g)/g$ for the O(2), O(3), and O(4) models. The results are listed in Tables II, III, and IV. They are as follows.

1. *O(2) model*

For the logarithmic derivative of $F(x)$, there is consistent evidence of a pole with

$$x_c = 1.6 \pm 0.2 . \tag{4.11}$$

The convergence of the residues is slow, but we estimate (with little confidence)

$$\rho = 2.2 \pm 0.5 . \tag{4.12}$$

The analysis of $\beta(g)/g$ also indicates a pole at $x_c = 1.7 \pm 0.2$ with a residue $\rho' = 1.2 \pm 0.5$.

2. *O(3) model*

The analysis for $F(x)$ indicates a pole at low order which disappears when higher orders are included. There is *no* evidence for a phase transition.

The analysis for $\beta(g)/g$ indicates the absence of a pole at finite positive x. The odd couple of poles can be regarded as accidental.

3. *O(4) model*

The situation is the same as for the O(3) model.

TABLE III. Same as Table II, for the O(3) model.

	(a)				(b)		
N	$[N/N-1]$	$[N/N]$	$[N/N+N]$	N	$[N/N-1]$	$[N/N]$	$[N/N+1]$
0			4.5(1.5)	0			
1		6.15(2.81)	•••	1		•••	25.7(7.94)
2	9.51(10.4)	•••	•••	2	•••	•••	
3	•••			3	4.42(−0.49)		

TABLE IV. Same as Table II, for the O(4) model.

N	$[N/N-1]$	$[N/N]$	$[N/N+1]$	N	$[N/N-1]$	$[N/N]$	$[N/N+1]$
0			9.60(1.60)	0			···
1		19.6(6.66)	···	1		···	
2	···	···	···	2	···	3.57(−0.027)	···
3	···			3	19.7(−16.8)		

4. *Ising model*

The logarithmic derivative of $F(x)$ is exactly $(x-1)^{-1}$. Every Padé approximant beyond first order gives the position and residue of the pole exactly.

In summary, the results of the Padé approximant test are in good overall agreement with those of the ratio tests.

We conclude that the O(3) and O(4) models always reside in the strong-coupling phase. However, we have strong evidence of a transition in the O(2) model occurring at $x_c = 1.6 \pm 0.2$.

Our results are marginally consistent with a simple algebraic zero of the O(2) model's mass gap at x_c, with a critical index $\rho = 2.1 \pm 0.5$. In conventional statistical-mechanics terminology this means that the correlation length ξ should have an algebraic singularity at the critical point with the critical index $\nu = 2.1 \pm 0.5$. However, Kosterlitz[5] has argued quite convincingly that ξ should have an *essential* singularity,

$$\xi \underset{x \to x_c}{\sim} \exp[b(x_c - x)^{-1/2}] . \tag{4.13}$$

It is interesting to see if our strong-coupling expansions favor Eq. (4.13) more strongly than an algebraic singularity. A direct test is given by the value of the β function critical index ρ'. Observe that if the mass gap vanishes exponentially,

$$F \underset{x \to x_c}{\sim} \exp[-b'(x_c - x)^{-\sigma}] , \tag{4.14}$$

then the β function should have a singular piece,

$$[\beta(g)/g]^{-1} \underset{x \to x_c}{\sim} \frac{2b'\sigma x_c}{(x_c - x)^{1+\sigma}} . \tag{4.15}$$

So, the relationship between ρ' and σ is simply $\rho' = 1 + \sigma$. In summary, if there is a simple algebraic singularity in the correlation length, then $\rho' = 1$ exactly; but, if the form found by Kosterlitz is correct than $\rho' = 1.5$. Unfortunately, our estimate (i.e., $\rho' = 1.2 \pm 0.5$) is sufficient to decide between these two possibilities. The slow convergence of our ratio test and Padé-approximant results can be construed as evidence for an exponential singularity. In the next section we shall argue that this is probably the case and that Kosterlitz's result is favored by our series results.

V. THE β FUNCTIONS FOR ALL COUPLINGS

1. *Ising model*

We include this result because it is exact and it serves as a reference for interpreting our other results. Since $F = 2(1-x)$, we have from Eq. (3.4)

$$\beta(g) = \left(\frac{1-x}{1+x}\right) g , \tag{5.1}$$

where $x = 2/g^2$. Equation (5.1) is plotted in Fig. 6. As written, Eq. (5.1) is meaningful above and at the phase transition $x_c = 1$.

2. *O(2) model*

The strong-coupling expansion of $\beta(g)/g$ is recorded in Table I to eighth order in $x = 2/g^2$. We wish to extrapolate this series into the intermediate coupling region ($x \sim 1-2$) to search for the

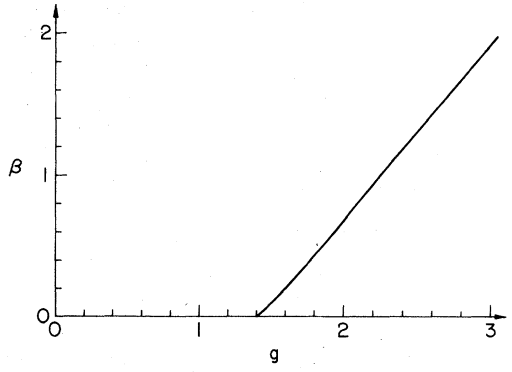

FIG. 6. The β function for the Ising model.

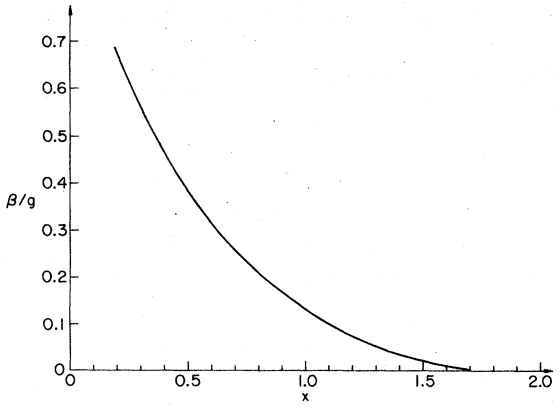

FIG. 7. $\beta(g)/g$ vs $x=2/g^2$ for the O(2) model.

phase transition we have found in previous sections. Since the coefficients in the series oscillate in sign, it is sensible to do this extrapolation with a Padé approximant. In particular, we form the [4, 4] approximant

$$\beta(g) = \left(\frac{1-0.1413x-0.2589x^2-0.1662x^3+0.09704x^4}{1+1.8587x+9584x^2+0.1664x^3-0.07654x^4}\right)g, \tag{5.2}$$

which is plotted in Fig. 7. Note the appearance of the phase transition at $x_c=1.7$ ($g_c=1.08$). Since *all* of our methods of searching for the phase transition in the O(2) model give this value for the transition point, we feel quite confident about it. In addition, if less terms in the series for $\beta(g)$ were used and the [3, 3] Padé approximant were formed, for example, essentially the same value for x_c would have been found.

Now we can address Kosterlitz's proposal that the correlation length diverges with an essential singularity at the critical point. Since the plot of β/g vs x is definitely concave upward, our analysis supports his result. In fact, if that curve is fit with a single power for $x \approx x_c$, one finds that

$$\beta(g)/g \approx 0.232(x_c - x)^{1.5} \tag{5.3}$$

provides a good interpolation formula for $x_c - x \leq 0.7$. Equation (5.3) is distinctly better than other powers such as $(x_c-x)^{1.3}$ or $(x_c-x)^{1.7}$ over that or similar ranges of x. Of course, Eq. (5.3) has precisely the form suggested by Kosterlitz.[5] We feel that this agreement is quite interesting. We interpret it as evidence for an essential singularity in the mass gap and site that as the reason for the slow convergence of the slopes observed in the ratio tests presented in previous sections.

3. O(3) model

Again we wish to obtain a plot of $\beta(g)$ for all g from our strong-coupling series. From previous sections we know that there is no tendency for β to vanish at finite x. However, β should vanish at $x=\infty$ ($g=0$). Then weak-coupling perturbation theory is applicable and two-loop calculations give[8]

$$\beta(g) = (N-2)\frac{g^2}{2\pi} + (N-2)\frac{g^3}{4\pi^2} + \cdots \tag{5.4}$$

for O(N). We would like to use the weak- and strong-coupling series to map out $\beta(g)$ for all coupling.[21] In particular, we would like to see that the two expansions match numerically in the intermediate coupling region and that a reasonable and smooth $\beta(g)$ can be deduced.

First, let us give more precise evidence of the fact that the strong-coupling series indicate a zero at $x=\infty$ ($g=0$). Consider the O(3) series

$$\beta(g)/g = 1 - \tfrac{2}{3}x + 2.963\times10^{-1}x^2 - 1.2284\times10^{-1}x^3 + 5.1516\times10^{-2}x^4 - 2.1459\times10^{-2}x^5 + 8.8659\times10^{-3}x^6. \tag{5.5}$$

We map the point $x=\infty$ to the unit disc by making a Moebius transformation which leaves the origin

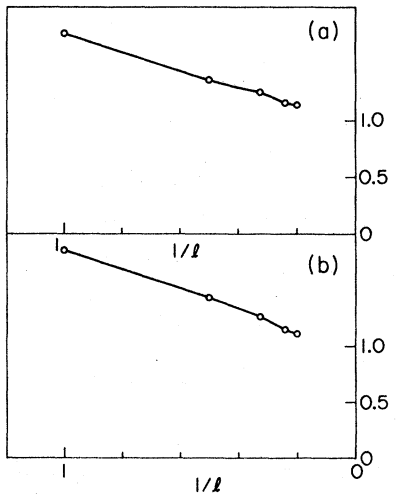

FIG. 8. Ratio tests for the logarithmic derivative of $\beta(g)/g$ as a function of z for (a) O(3) model and (b) O(4) model.

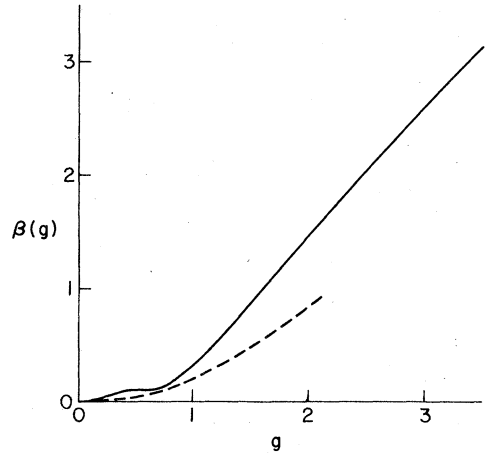

FIG. 9. The solid line is the β function obtained from the strong-coupling expansion using a [2,3] Padé approximant. The dashed curve is the weak-coupling curve for the O(3) model.

fixed,

$$z = \frac{x}{1+x} \,. \tag{5.6}$$

In terms of z, the series becomes

$$\beta(g)/g = 1 - \tfrac{2}{3}z - 3.7037\times10^{-1}z^2 - 1.9691\times10^{-1}z^3 - 9.4781\times10^{-2}z^4 - 3.3916\times10^{-2}z^5 + 3.1455\times10^{-3}z^6 \,. \tag{5.7}$$

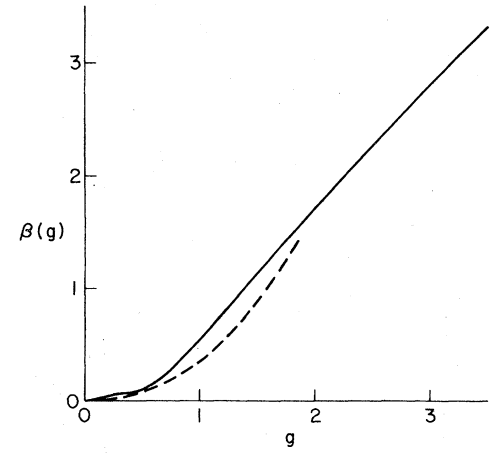

FIG. 10. Same as Fig. 9, for the O(4) model.

The point of making the Moebius transformation is that we can search for the radius of convergence of Eq. (5.7). In particular, we take the logarithmic derivative of Eq. (5.7),

$$-\tfrac{2}{3} - 1.1852z - 1.6278z^2 - 2.0346z^3 - 2.4254z^4 - 2.8071z^5 \tag{5.8}$$

and apply the ratio test. As shown in Fig. 8 we have good evidence for a pole in the logarithmic derivative at $z_c = 1.03 \pm 0.10$. This point is consistent with $z=1$ which corresponds to $x=\infty$. Although this analysis is certainly crude, it is quite suggestive.

Now we will use the strong-coupling expansion and produce an interpolating formula for $\beta(g)$ which satisfies the following two boundary conditions:

1. at large g, $\beta(g) \sim g$,
2. at small g, $\beta(g) \sim g^2$.

The first fact is, of course, implicit in the strong-coupling analysis and can be read off Eq. (5.5), for example. The second fact follows from conventional weak-coupling expansions and is made precise in Eq. (5.4). To make the interpolation formula we consider the strong-coupling series for $[\beta(g)/g]^2$ and form its [2,3] Padé approximant. This procedure satisfies the conditions 1 and 2 above and the resulting curve of $\beta(g)$ vs g is shown in Fig. 9. We have several observations about this curve:

1. The [2,3] Padé approximant matches onto the weak-coupling perturbative result in the intermediate coupling region $g \approx 1$ quite accurately. This constitutes good evidence that the system exists in a single phase.
2. The numerical match between the weak-coupling expansion and the [2,3] Padé approximant is good even near the origin.
3. The intermediate coupling region (where neither expansion method is particularly accurate) appears to be quite narrow. The transition from weak-coupling behavior to strong-coupling behavior appears to occur at $g \approx \frac{3}{4}$.
4. The wiggles in the interpolation formula near the origin are probably not reliable since they vary as different calculational procedures are used (see Sec. VI).

4. O(4) model

This analysis follows the O(3) discussion quite closely. In this case the series in the variable z for the logarithmic derivative of $\beta(g)/g$ is

$$-\tfrac{1}{3} - 0.625z - 0.88263z^2 - 1.112z^3 - 1.3173z^4 - 1.5014z^5$$

and the results of the ratio test are shown in Fig.

8. The [2,3] Padé interpolation curve for $\beta(g)$ is shown in Fig. 10 along with the weak-coupling expansion. We note that the compatibility of the two curves is better for O(4) than for O(3), and that the transition between weak and strong coupling has moved closer to the origin $g \approx \frac{1}{2}$.

VI. TWO-POINT PADÉ APPROXIMANTS FOR THE β FUNCTIONS OF THE O(3) AND O(4) MODELS

The interpolating forms presented in Figs. 9 and 10 do not use all the information known about these theories's β functions in quantitative detail. In this section we will present interpolating formulas which lead to Eq. (5.4) for small g and reproduce the strong-coupling expansions listed in Table I for the non-Abelian models. A systematic method exists for doing this. It is called the N-point Padé approximant and we will review it in a form suitable for our application.[22]

Suppose that we know N terms of an expansion of the function F about the origin,

$$F(z)=\sum_{n=0}^{N-1} a_n z^n + O(z^N), \tag{6.1a}$$

and M terms of the expansion of F around infinity,

$$F(z)=z^L \sum_{n=0}^{M-1} b_n z^{-n} + O(z^{L-M}). \tag{6.1b}$$

Then it is possible to form the $[P/Q]$ Padé approximant to $F(z)$,

$$[P/Q](z)=\frac{p_0+p_1 z+\cdots+p_P z^P}{1+q_1 z+\cdots+q_Q z^Q}, \tag{6.2}$$

where $P-Q=L$ and $P+Q+1=N+M$. The coefficients p_i and q_i are determined from the following requirements:

(a) The series expansion of $[P/Q]$ about the origin should agree with Eq. (6.1a) up to $O(z^N)$,

$$\begin{aligned} p_0 &= a_0, \\ p_1 &= a_0 q_1 + a_1, \\ &\cdots \\ p_P &= a_0 q_P + a_1 q_{P-1} + \cdots + a_P, \\ 0 &= a_0 q_{P+1} + a_1 q_P + \cdots + a_{P+1}, \\ &\cdots \\ 0 &= a_{N-Q-1} q_Q + \cdots + a_{N-1}, \end{aligned} \tag{6.3a}$$

for the case $N > Q > P > M$.

(b) The series expansion of $[P/Q]$ about infinity should agree with Eq. (6.1b) up to $O(z^{L-M})$,

$$\begin{aligned} p_P &= b_0 q_Q, \\ p_{P-1} &= b_0 q_{Q-1} + b_1 q_Q, \\ &\cdots \\ p_{P-M+1} &= b_0 q_{Q-M+1} + \cdots + b_M q_Q. \end{aligned} \tag{6.3b}$$

Equations (6.3a) and (6.3b) comprise a total of $N+M=P+Q+1$ linear equations which give unique values to the Padé coefficients p_i and q_i. Clearly this construction is a natural generalization of the usual Padé approximant. It is particularly suited to the problem at hand since the analysis in the previous sections of this article suggest that the O(3) and O(4) models are single-phase systems. Hence, a smooth interpolation between weak and strong coupling should exist. The two-point Padé approximant provides a well-defined, systematic method of doing this.[23]

We have calculated the two-point Padé approximants for the β functions of the O(3) and O(4) models. The results are shown in Figs. 11 and 12. The coefficients of the [7/8] Padé approximants

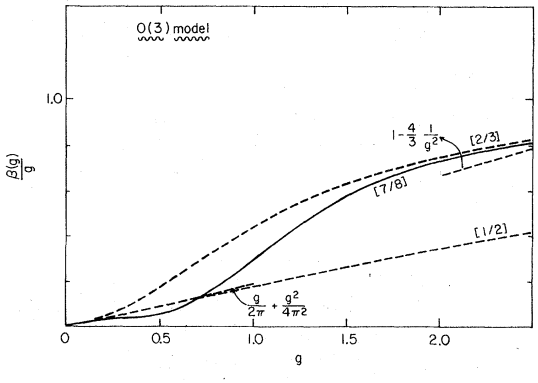

FIG. 11. Two-point Padé approximants for $\beta(g)/g$ of the O(3) model plotted as a function of g. The best approximant is $[\frac{7}{8}]$. Also shown are the weak- and strong-coupling expansions.

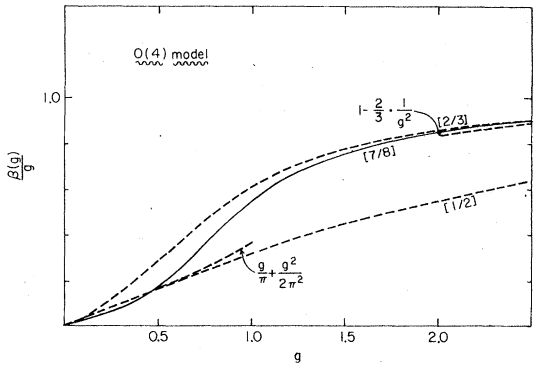

FIG. 12. Same as Fig. 11 except for the O(4) model.

TABLE V. The coefficients of the [7/8] two-point Padé approximants as defined in Eq. (6.2) for the function $\beta(g)/g$ for the O(3) and O(4) models. The variable z in Eq. (6.2) is $1/g$ in this application.

	O(3) model			O(4) model	
i	p_i	q_i	i	p_i	q_i
0	1	1	0	1	1
1	0.020 249	0.020 249	1	0.064 665	0.064 665
2	−0.295 35	1.038	2	−0.191 01	0.475 65
3	0.022 397	0.049 397	3	0.015 944	0.059 053
4	0.083 999	0.282 79	4	0.052 396	0.063 937
5	−0.020 634	0.021 229	5	$-7.209\,8\times10^{-3}$	0.012 4
6	$4.804\,3\times10^{-5}$	0.129 6	6	5.572×10^{-5}	0.022 63
7	$5.321\,2\times10^{-3}$	-5.019×10^{-3}	7	$1.233\,9\times10^{-3}$	-4.419×10^{-4}
8	...	0.033 433	8	...	$3.376\,4\times10^{-3}$

are collected in Table V.

Inspecting the figures, we learn the same semiquantitative facts that were pointed out in Sec. V. For example, in the O(4) model $\beta(g)/g$ grows from 0.17 at $g=0.5$ to 0.78 at $g=1.5$. So, the transition from weak- to strong-coupling behavior has essentially occurred over a region of width $\Delta g \approx 1$. And, as in all of our analyses, there is no evidence for a zero in $\beta(g)$ at any value of g different from zero.

VII. DISCUSSION AND CONCLUSIONS

Let us collect together our conclusions for the various models.

1. O(2) model

We have strong evidence for a phase transition at the coupling $x_c=1.7$. We favor an exponential singularity in the mass gap with a critical index in agreement with the Kosterlitz renormalization group. However, higher-order calculations are necessary to establish this result with confidence.

2. O(3) model

We have strong evidence that this theory only exists in the strong-coupling phase. A Padé approximant extrapolation of the β function from strong coupling numerically matches with weak-coupling perturbation theory in the intermediate coupling region. The transition from weak- to strong-coupling behavior appears to be quite abrupt. This result agrees with Migdal recursion relation.[7,10] The transition region occurs near $g \approx \frac{5}{4}$.

3. O(4) model

The results are similar to the O(3) model. The matching in the intermediate coupling region between the strong- and weak-coupling expansions is somewhat better than for the O(3) model and the crossover occurs nearer the origin ($g \approx \frac{1}{2}$). Although the O(3) model has instantons while the O(4) model does not, we do not find any dramatic differences between them. We had expected that the instantons of the O(3) model would introduce additional disordering at small coupling and lead to a narrower transition region than in the O(4) model. Instead the transition region is narrower and clearer for the O(4) model than the O(3) model. Apparently the extra disorder in the additional spin-wave modes of the O(4) model is numerically more significant than the extra disorder in the instantons of the O(3) model.

In summary, our series clearly distinguish the Abelian from the non-Abelian models. Given a finite amount of work, it is our opinion that Hamiltonian strong-coupling expansions are a more reliable way of searching for phase transitions than the traditional high-temperature expansions. It may be interesting and useful to apply the Hamiltonian methods to other models of interest to the statistical mechanician.

ACKNOWLEDGMENTS

C. J. H. would like to thank Dr. N. E. Frankel, Professor C. J. Thompson, and Dr. M. N. Barber for stimulating and informative discussions. J. B. K. and L. S. thank their colleagues at Illinois, Stanford, and SLAC for discussions. The work of J. B. K. was supported in part by the A. P. Sloan Foundation and in part by the National Science Foundation under Grant No. NSF PHY 77-25279.

[1]J. Kogut and L. Susskind, Phys. Rev. D 11, 395 (1975).
[2]See, for example, H. E. Stanley and T. A. Kaplan, Phys. Rev. Lett. 17, 913 (1966). More elaborate series analyses of the classical O(3) model can be found in A. J. Guttmann, J. Phys. A 11, 545 (1978).
[3]N. D. Mermin and H. Wagner, Phys. Rev. Lett. 17, 1133 (1966).
[4]J. M. Kosterlitz and D. J. Thouless, J. Phys. C 6, 1181 (1973).
[5]J. M. Kosterlitz, J. Phys. C 7, 1046 (1974).
[6]A. M. Polyakov, Phys. Lett. 59B, 79 (1975).
[7]A. A. Migdal, Zh. Eksp. Teor. Fiz. 69, 810 (1975) [Sov. Phys.—JETP 42, 413 (1976)].
[8]E. Brezin and J. Zinn-Justin, Phys. Rev. B 14, 3110 (1976).
[9]A. Zamolodchikov and Al. Zamolodchikov, Nucl. Phys. B133, 525 (1978); Zh. Eksp. Teor. Fiz. Pis'ma Red. 26, 608 (1977) [JETP Lett. 26, 457 (1977)].
[10]L. P. Kadanoff, Ann. Phys. (N.Y.) 100, 359 (1976).
[11]A. A. Belavin and A. M. Polyakov, Zh. Eksp. Teor. Fiz. Pis'ma Red. 22, 503 (1975) [JETP Lett. 22, 245 (1975)].
[12]A. M. Polyakov, Phys. Lett. 72B, 224 (1977).
[13]K. G. Wilson and J. Kogut, Phys. Rep. 12C, 75 (1974).
[14]E. Fradkin and L. Susskind, Phys. Rev. D 17, 2637 (1978).
[15]See, for example, the review article by J. B. Kogut, in *Many Degrees of Freedom in Particle Theory*, proceedings of the 8th International Summer Institute of Theoretical Physics, Bielefeld, 1976, edited by H. Satz (Plenum, New York, 1978), Vol. 2, p. 275.
[16]M. E. Rose, *Elementary Theory of Angular Momentum* (Wiley, New York, 1957).
[17]L. C. Biedenharn, J. Math. Phys. 2, 433 (1961).
[18]A. R. Edmonds, *Angular Momentum in Quantum Mechanics* (Princeton Univ. Press, Princeton, N. J., 1960).
[19]P. Pfeuty, Ann. Phys. (N.Y.) 57, 79 (1970).
[20]Slow convergence and/or oscillations in the slopes can be caused by singularities at negative x. This possibility limits the usefulness of linear extrapolations and slopes in general. Methods exist for softening these effects and will be considered in a forthcoming paper containing some high-order series. In addition, the Padé-approximant test discussed below is not sensitive to this limitation.
[21]The perturbative β function is calculated using relativistic Feynman diagrams, a cutoff procedure very different from that used here. However, since the β function is universal (through two loops) we are justified in comparing with it near $g=0$.
[22]The N-point Padé approximant is discussed in Chapter 8 of *Essentials of Padé Approximants* by George A. Baker, Jr. (Academic, New York, 1975).
[23]Other interpolation methods have been suggested for the susceptibility of the O(3) model. See D. S. Fisher and D. R. Nelson, Phys. Rev. B 16, 2300 (1977).